Simulations of Spontaneous Phase Transitions in Large, Deeply Supercooled Clusters of SeF_6

Yaroslav G. Chushak and Lawrence S. Bartell*

Department of Chemistry, University of Michigan, Ann Arbor, Michigan, 48109

Received: August 10, 1999; In Final Form: October 22, 1999

The crystallization and subsequent solid-state transitions in a series of large clusters of SeF_6 of two sizes have been studied by molecular dynamics simulations at constant temperature. Several diagnostic methods were applied to monitor molecular details of the clusters' structures and their evolution with time. The behavior of 12 liquid clusters with 725 molecules and 10 with 1722 molecules was examined at 140 and 130 K. During the nanosecond runs of the simulations all of these clusters froze, initially to the bcc or a related but distorted structure. At the higher temperature all but one of the larger clusters underwent a transition to the monoclinic structure whereas all but one of the smaller clusters remained bcc. At the lower temperature all of the smaller clusters ultimately transformed, usually quite abruptly, to the monoclinic structure. In the case of the larger clusters a transition to the monoclinic phase was observed at 140 K whereas at 130 K, besides the monoclinic structure, the orthorhombic or a mixture of orthorhombic and monoclinic phases was obtained in a few clusters. Many of the larger frozen clusters were polycrystalline while the smaller ones were single crystals. How these results relate to Kashchiev's criterion for mononuclear vs polynuclear growth is discussed, and the time dependence of crystal growth was found to agree well with the Kolmogorov−Johnson−Mehl−Avrami equations. Growth rates of the bcc phase were in reasonable agreement with Turnbull's theory. Simulations of solid-state transitions from clusters prepared to have a well-ordered bcc configuration clearly indicate a lower nucleation rate for the low-energy phase than in a cluster with grain boundaries and/or solid−liquid interfaces. A striking result was that nucleation invariably occurred at or near the clusters' surfaces despite the fact that surfaces of clusters tend to be disordered and melt at significantly lower temperatures than their cores. Such a behavior has also been reported for simulations of monatomic clusters.

Introduction

In a program of examining homogeneous nucleation in the freezing and solid-state transitions of highly supercooled phases, new features continue to appear as our systems of large molecular clusters are made larger. These systems have most commonly consisted of chalcogen hexafluorides, the subject of the present paper. Our initial 150-molecule clusters were constructed to be considerably larger than the critical nuclei predicted by the classical theory of nucleation.[1,2] Nevertheless, these clusters turned out to be far too small to characterize critical nuclei.[2] Indeed, what exactly constitutes a critical nucleus has been unclear. As a liquid supercools, structural fluctuations occur that lead to aggregates resembling the bcc structure, the phase to which the liquid normally freezes. Although such aggregates meet a Voronoi criterion to be described subsequently, they are flickering filaments or sheets so thin that all molecules in them are in contact with the liquid. The total number of contiguous molecules in these aggregates may be considerably greater than the size of a critical nucleus implied by the classical nucleation theory, but their development with time does not give a clear signal of when the onset of nucleation can be considered to have occurred. In the previous paper of this series,[3] a much more easily recognized indicator of the onset of nucleation was found and will be adopted in the present work. What sites in a cluster favor nucleation and whether the freezing of liquid clusters is mononuclear or polynuclear will be examined in clusters considerably larger than those selected in our previous reports. Solid-state transitions are also studied along with growth rates of the new phase in the old.

Computational Details

Molecular dynamics simulations were performed on clusters containing 881 and 2085 molecules of SeF_6. Molecules were taken to be rigid octahedra with Se−F bond lengths of 1.67 Å.[4] Simulations were carried out at constant temperature using a seven-site intermolecular interaction function based on pairwise-additive Lennard-Jones potential functions with partial charges assigned to the atoms. The potential function had been constructed to optimize crystallographic data and has been described in detail elsewhere.[1,5]

For both cluster sizes, an initial, approximately spherical cluster was constructed to be in its low-temperature monoclinic phase. Both were heated from 100 to 280 K with temperature steps of 10 K, and equilibrated at each temperature for 4000 time steps of 7 fs (881 molecules) and for 10 000 time steps (2085 molecules). This time span appears to be long enough to establish equilibrium for temperatures not too close to the phase transition temperature. In the vicinity of melting transition the temperature step was reduced to 5 K and the equilibration time was doubled. At every stage, velocities were rescaled at each step in order to approach the desired temperature. The final configuration at 230 K was additionally equilibrated for 40 000 time steps (280 ps), generating along the way 12 saved configurations for an 881-molecule cluster and 10 saved configurations for a 2085-molecule to serve as independent

10.1021/jp992818g CCC: $18.00
Published on Web 11/30/1999

TABLE 1: Voronoi Polyhedra Found in 1722-Molecule Clusters of SeF_6

	index				percent	
no. of faces	n_3	n_4	n_5	n_6	bcc	mono
12	0	4	4	4	4	5
13	0	3	6	4	3	2
13	0	5	2	6	10	10
14	0	4	4	6	1	11
14	0	6	0	8	79	60
15	0	5	2	8	0	3
other					3	9

starting configurations for cooling runs. Past experience indicated that intervals of 21 ps between the saved configurations was sufficient for the purpose. During the heating and equilibration at 230 K, some of the molecules evaporated from the clusters and final configurations contained different numbers of liquidlike molecules. Therefore, to make the members of the set equivalent, approximately spherical configurations were constructed by trimming down each cluster to a size of 725 molecules (smaller cluster) or 1722 molecules (larger cluster). Starting from 230 K, each configuration was cooled to either 140 or 130 K in decrements of 20 K, spending 1000 time steps at each temperature. The corresponding cooling rate was 3.2×10^{12} K/s. All configurations generated for production runs were still liquid, even though deeply supercooled, as determined by the absence of solidlike nuclei (see below) large enough too initiate crystallization.

Production runs were carried out at both 140 and 130 K. Durations of runs were 1 ns. Phase transitions were recognized from the evolution of configurational energy and by structure analyses described in the next section.

Structure Analysis

In order to identify molecules as belonging to either liquid- or solidlike regions, we used the widely adopted technique based on Voronoi polyhedra.[6−8] The principal crystalline phases encountered in the runs were bcc and monoclinic (space group $C2/m$). For a perfect bcc crystal the Voronoi polyhedron has 14 faces, six with four edges and eight with 6 edges (designated 0608), and this polyhedron has been shown to be stable against small thermal distortions in instantaneous configurations of systems of monatomic molecules.[6] Thermal amplitudes of vibrations in bulk plastically crystalline hexafluorides are large, however, and additional distortions can occur in clusters where a large proportion of molecules are in the surface or close to it. Those in the surface itself cannot even be assigned Voronoi polyhedra. In an earlier study of chalcogen hexafluoride clusters in this laboratory[1] it was found in simulations that several Voronoi polyhedra besides the ideal (0608) example occurred in clusters that had been constructed to have ideal structures and then subjected to normal thermal agitation. Therefore, a reference set of six Voronoi polyhedra encountered in such clusters was adopted to identify solidlike molecules. Since the translational differences between the bcc and monoclinic structures are minor, the same set of Voronoi polyhedra could be used in both cases. In the final configurations of completely crystallized clusters, only 3−5% of bcc and 5−10% of monoclinic molecules in the clusters cores fell outside of this set (see Table 1).

Once molecules in the supercooled liquids have been identified as solidlike, they are considered to be members of embryos, the precursors of nuclei. If such a molecule is a neighbor of another solidlike molecule it is assigned to the same embryo. The cutoff distance for neighbors was chosen to be 7.2 Å, the position of the first minimum in the pair correlation function of the bcc solid. Embryos spontaneously forming at the deep supercooling of the runs are initially extremely ramified with constituent molecules all in direct contact with the surrounding liquid. These embryos are ephemeral, fluctuating in shape and size, and they often contain many more molecules than critical nuclei are predicted to possess according to the classical theory of homogeneous nucleation.[2] Although these forerunners of nucleation are readily recognized, the unfolding of their history does not provide a satisfactory basis for analyzing nucleation rates. What is needed is a more robust criterion of when meaningful nucleation begins. We have found what appears to meet that criterion by defining bulklike solid molecules to mean those molecules which pass the Voronoi test and, in addition, which are surrounded by at least 12 solid neighbors.[3] These bulklike pockets do appear abruptly, usually followed by rapid growth. Note that the minimum size of such pockets, at 13 molecules, is already about twice as large as critical nuclei at the ambient supercooling of our runs according to the classical theory of homogeneous nucleation.

Although Voronoi polyhedra clearly distinguish solidlike molecules from those of the liquid, they are ineffective in recognizing the transition from the bcc to the monoclinic phase. In this transition, it is molecular reorientations rather than translations that play the principal role. Even in bulk samples the bcc phase of chalcogen hexafluorides is plastically crystalline, owing to a large disorder in molecular orientations.[9] This disorder is a consequence of "orientational frustration" arising from the reluctance of the negatively charged fluorines of neighboring molecules to point directly toward each other as they would in a "perfect" bcc crystal. The lower energy and more ordered monoclinic phase differs from its bcc counterpart by a 60° rotation of $^1/_3$ of the molecules which leads to a more efficient packing of fluorines.[10,11] Perhaps the most convenient procedure for portraying orientations of molecules in clusters is the Pawley projection[12] (plots of the projections of bond directions on a hemisphere over a cluster). On the other hand, this technique is not well suited for identifying whether an individual molecule is in a bcc or monoclinic environment. To this end we adopt a function $Q(\theta)$ introduced by Xu[13,14] to characterize the molecular (or local) orientational distribution. It is a normalized histogram of the angles between the bonds of molecule i and those of its neighbors, j, or

$$Q_i(\theta) = \frac{1}{N_i N_b^2} \left\langle \sum_{j=1}^{N_i} \sum_{\alpha,\beta=1}^{N_b} \delta[\theta - (\theta_{\alpha\beta})_{ij}] \right\rangle \tag{1}$$

where N_i is the number of neighbors of the ith molecule, N_b is the number of bonds in the molecule, and $(\theta_{\alpha\beta})_{ij}$ is the angle between the bond α in molecule i and bond β in molecule j, calculated via the relation

$$(\theta_{\alpha\beta})_{ij} = \arccos[(\mathbf{n}_\alpha)_i \cdot (\mathbf{n}_\beta)_j] \tag{2}$$

in which $(\mathbf{n}_\alpha)_i$ and $(\mathbf{n}_\beta)_j$ are the unit vectors along the bonds involved. The total orientational distribution function is defined to be

$$Q(\theta) = \frac{1}{N} \sum_{i=1}^{N} Q_i(\theta) \tag{3}$$

In Figure 1 the pair correlation functions $g(r)$ and the orientational distribution functions $Q(\theta)$ are illustrated for SeF_6 clusters in the bcc and monoclinic phases. The peak positions of the

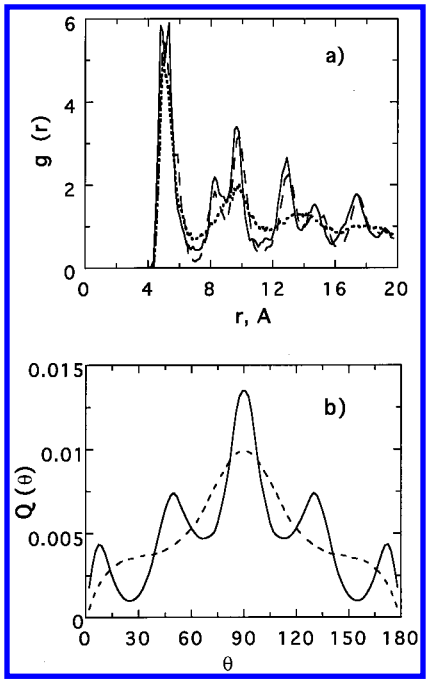

Figure 1. (a) Pair-correlation functions $g(r)$ and (b) orientational angular distribution functions $Q(\theta)$ for the 725-molecule cluster at 130 K. Solid curves, for the monoclinic structure; dashed lines, for the bcc structure. Dotted curve in (a), the initial liquid phase.

pair correlation functions in the monoclinic and bcc configurations are similar, consistent with the fact that the translational reorganization of the molecules is not large in the transition from the bcc structure to the monoclinic. On the other hand, the orientational distribution function $Q(\theta)$ for monoclinic can be seen to be very different from that for the bcc structure. There are more peaks for the monoclinic structure than for the bcc, and they are sharper because the molecular orientations are more ordered. These properties in $Q(\theta)$ (which also are observed in the $Q_i(\theta)$ for individual molecules) can be used to identify whether an individual molecule is in a bcc or monoclinic environment. That is, a molecule is in monoclinic environment if the ratio $Q_i(\theta=10°)/Q_i(\theta=20°) > 3.0$.

Results

Temperatures of phase transitions during the heating of clusters were recognized from the caloric curves *U(T)* and from the temperature dependence of the volume per molecule (Figure 2). The latter property gives a more conspicuous indication of the transitions than the former. Clusters with 881 molecules transformed from the monoclinic to the body-centered cubic phase at about 150 K and melted at 200 K. The solid-state transition for the larger cluster was observed at approximately 155 K and melting at 210 K. Transformations from the monoclinic to bcc structure took place over a temperature range of about 10 K while the range for the melting transitions was roughly 20 K. In Figure 3 we plot the monoclinic−bcc and melting transition temperatures as a function of $N^{-1/3}$, where N is the number of molecules in a cluster. In this figure we also included the data from our previous simulations for a 150-molecule cluster.[2] Although the experimental bulk melting point of 239 K[15,16] is well established, there is some disagreement about the solid-state transition temperature. Values from 128 to 173 K have been reported.[15−18] The size dependence of the melting transition temperature can be well represented by a straight line (Figure 3) that gives an extrapolated bulk value in fair agreement with the experimental value. The same is true

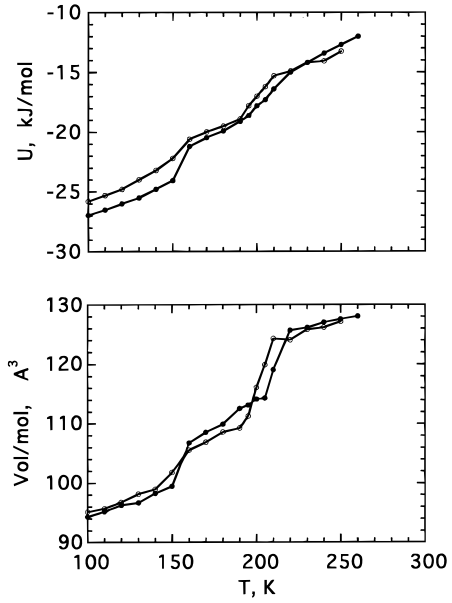

Figure 2. Temperature dependence of configurational energy per molecule and volume per molecule for SeF_6 clusters during heating stages. Open circles, 881-molecule; solid points, 2085-molecule clusters.

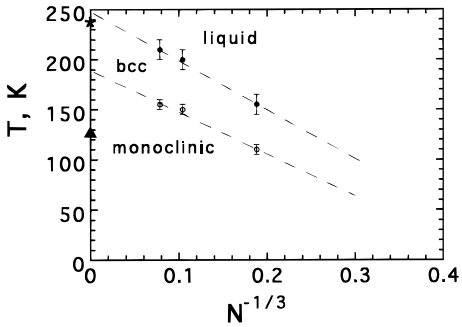

Figure 3. Computed monoclinic−bcc (open circles) and melting transition temperatures (solid circles) as a function of $N^{-1/3}$. For comparison the experimental melting point[15] (asterisk) and solid-state transition temperature[17,18] (solid triangle) are shown for the bulk material.

for the solid-state transformation temperature if we assume 173 K to be the bulk transition point.[15] On the other hand, some evidence[19] strongly favors 128 K as the temperature for the monoclinic−bcc phase transformation. In this case, the extrapolation in Figure 3 fails and fails badly. A similar failure was also found in computer simulations of the monoclinic−bcc transition in TeF_6[13] and SF_6[20] clusters. It has been suggested[21] that the misfit between the denser monoclinic structure and the bcc region leads to a significant stress that raises the apparent transition temperature. Furthermore, this stress increases as cluster size increases, leading to a spurious extrapolation.

Freezing and bcc−monoclinic transitions of sets of clusters with 725 or 1722 molecules have been investigated at 140 and 130 K. The following sections describe the behavior observed in simulations and also estimate growth rates. We treat the two cluster sizes in separate sections because the results are somewhat different. Nucleation rates and what can be inferred from them will be covered in a subsequent paper.

725-Molecule Clusters. During the nanosecond runs at 140 K, 11 of the 12 clusters froze to the bcc structure while one cluster quickly passed through a bcc stage and transformed to a monoclinic structure. Figure 4 shows the numbers of bulklike solid and monoclinic molecules as functions of time for all 12 runs. Pawley projections are presented in Figure 5. Included

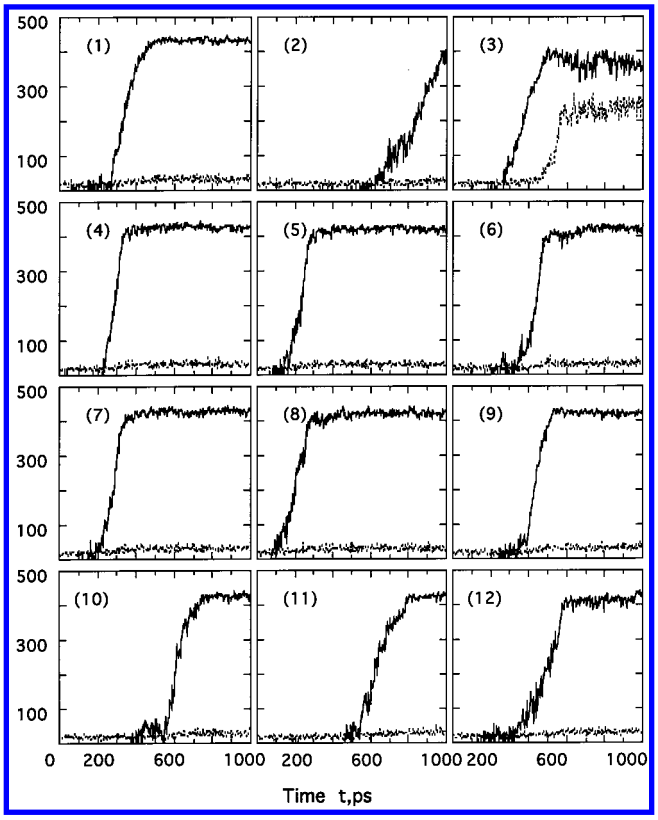

Figure 4. Time evolution of number of bulklike solid molecules (solid lines) and monoclinic molecules (dashed lines) for the 725-molecule clusters at 140 K.

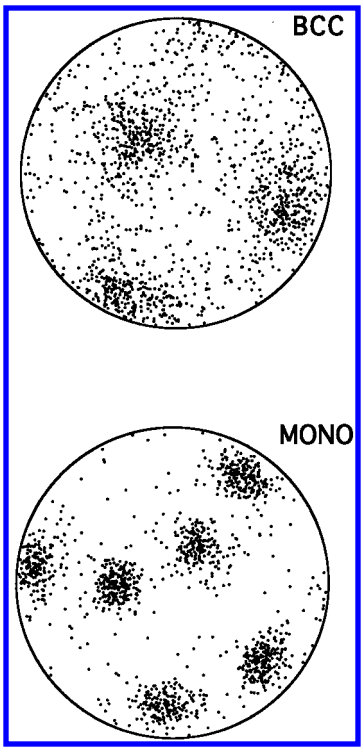

Figure 5. Pawley projections of bond directions of all the molecules in a typical 725-molecule cluster at 140 K in the bcc final configuration and for cluster no. 3 in the final monoclinic configuration.

are plots for the final configurations of cluster no. 3, which transformed to the monoclinic phase, and for a typical cluster which remained in the bcc phase. Only the core molecules (i.e., molecules that have 12 or more neighbors) are included in those pictures. Molecular orientations in the bcc phase are conspicuously disordered in the plastically crystalline bcc phase for reasons explained in the previous section. The orientations of molecules in the monoclinic phase can be seen to be more highly ordered and to add three additional patches of spots corresponding to the $^1/_3$ of the molecules which have reoriented by a 60° rotation about one of their 3-fold axes during the transformation.

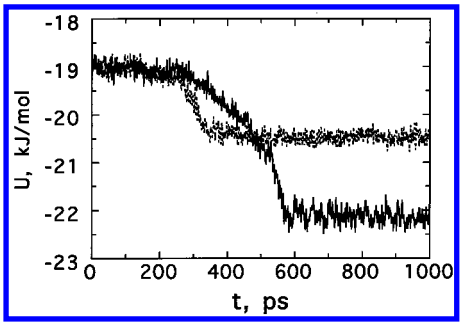

Figure 6. Time evolution of configurational energy of 725-molecule cluster no. 3 which transformed to monoclinic via bcc from the liquid (solid line) and cluster no. 4 (dashed line) which remained in the bcc structure during the crystallization at 140 K.

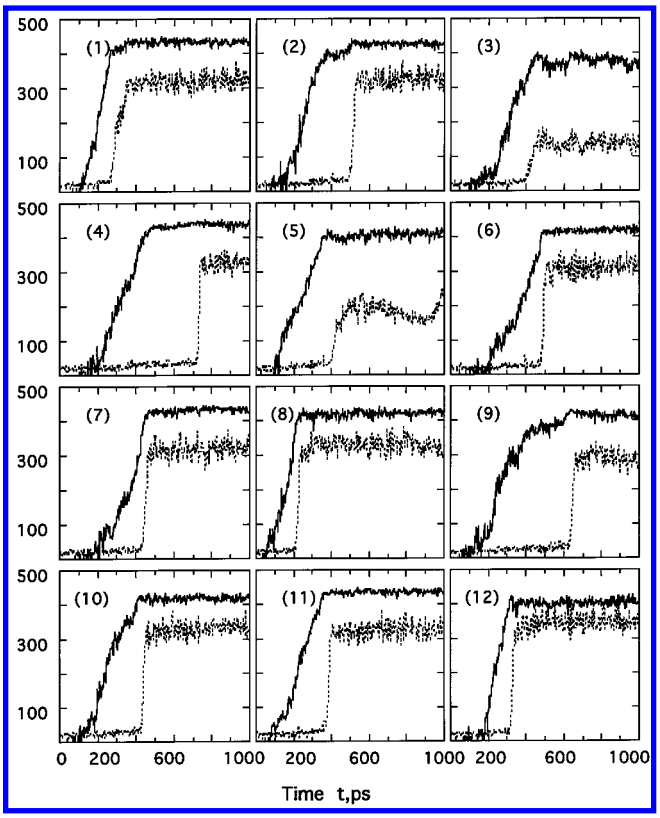

Figure 7. Same as in Figure 4 except at 130 K.

The evolution of the configurational energy for the cluster no. 3 which transformed to monoclinic and for the cluster no. 4 which did not, are shown in Figure 6. Although the monoclinic structure is more stable at this temperature, the transition from the bcc to the monoclinic phase is a process which involves the surmounting of a free-energy barrier. That is why only one cluster, by chance, transformed to the monoclinic structure at 140 K during the nanosecond runs of the present simulations. The situation is quite different at 130 K where, at the deeper supercooling and, hence, lower nucleation barrier, all 12 clusters ultimately transformed to the monoclinic phase. Figure 7 presents the numbers of bulklike solid and monoclinic molecules vs time at 130 K. Transitions to the monoclinic phase occurred most frequently when the number of bcc molecules reached its

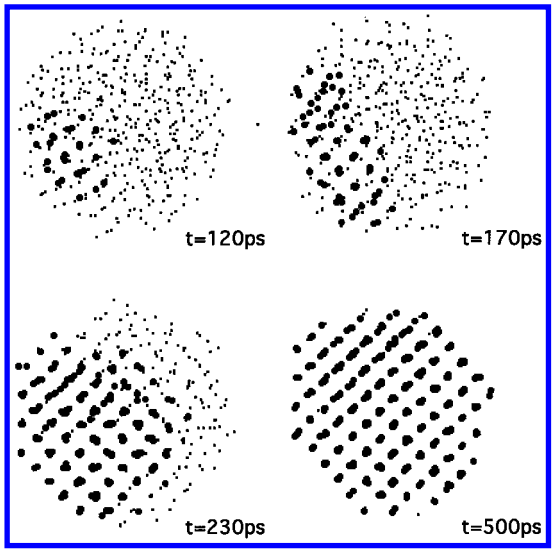

Figure 8. Projections of centers of mass of core molecules in 725-molecule cluster no. 1 during the crystallization at 130 K. Heavy dots identify the bulklike solid molecules.

maximum. Only for one cluster was a substantial time lag observed between the full transformation to bcc and the transition to monoclinic. Because freezing requires a major molecular translational reorganization, it is comparatively slow, usually taking 200−300 ps to complete, once freezing has begun. On the other hand, the solid-state transition from bcc to the monoclinic phase involves a more modest reorganization, namely the reorientation of only $^1/_3$ of molecules. For this process to be completed takes only about 30 ps.

It is worthwhile here to make a crude estimate of the rate of growth of the new phases during the phase changes. Since only the core molecules possess Voronoi polyhedra, of which there are roughly 440, the plots of Figure 7 show only the cluster cores. From the number density of the bcc phase found in the MD runs to be 0.0096 Å^{-3}, the radius of the core was calculated to be about 22.2 Å. Therefore, based on the transformation times in Figure 7, the growth rates during crystallization and the solid-state transition are estimated to be roughly 9 and 74 m s^{-1}, respectively, if it is assumed that nucleation started at the center of cluster.

Let us now see how the crystallization proceeds on the molecular scale. In the cluster images of Figure 8, molecules identified as in bulklike crystalline aggregates are represented by heavy dots to distinguish them from molecules in the diffuse interface and liquid (light dots). As an example, the freezing of cluster no. 1 at 130 K was chosen. Before the onset of crystallization, the cluster contained more than 100 molecules that passed the bcc Voronoi test, but the distribution of these molecules was very haphazard and all of them were in direct contact with the liquid. At ∼100 ps a bulklike bcc nucleus appeared and rapidly started to grow. One can readily see from Figure 8 that the nucleus has a more ordered crystalline structure than do the surrounding molecules. At ∼400 ps the cluster completely transformed to the bcc structure.

1722-Molecule Clusters. As shown in Figure 9, nine of the 10 liquid clusters at 140 K began to freeze to the bcc structure but soon underwent a transition to the monoclinic structure. The other cluster (no. 4) remained in the bcc structure during the entire nanosecond duration of simulations, a behavior rationalized in the next section. Displayed in Figure 10 are the plots corresponding to the histories of clusters at 130 K. All of the clusters, after passing through the bcc or bcc-like intermediate

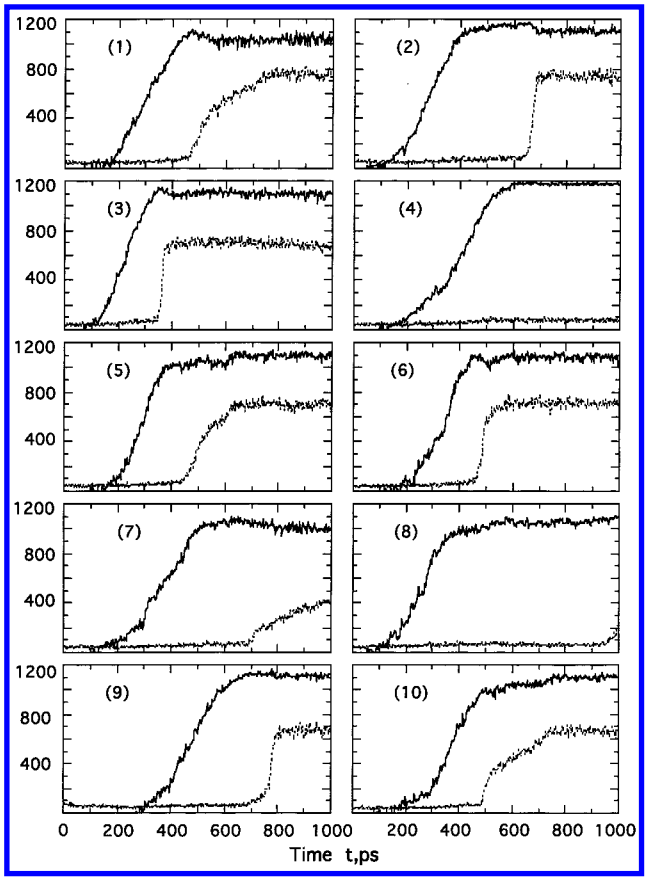

Figure 9. Time evolutions of number of bulklike solid molecules (solid lines) and monoclinic molecules (dashed lines) for the 1722-molecule clusters at 140 K.

structures, transformed, usually abruptly, to low-energy structures resembling monoclinic or orthorhombic phases. An analysis of the clusters' pair correlation functions (PCF) shows that cluster no. 2 has a distinctly different organization than monoclinic. It was identified as orthorhombic (space group *Pnma*). Some traces of the orthorhombic structure are also observed in the PCF of clusters no. 4 and no. 8 but they do not have a strong overall impact. Because of the different spatial arrangement of molecules in the orthorhombic phase compared with the bcc or monoclinic, the appearance of orthorhombic regions leads to a significant drop in the number of molecules passing our Voronoi test (see especially no. 2, Figure 10). Unfortunately, the orientational distribution functions for monoclinic and orthorhombic structures are nearly the same and therefore are not useful in distinguishing orthorhombic from monoclinic structures.

Because $^1/_3$ of molecules rotate about one of their 3-fold axes during the bcc−monoclinic transition while half reorient to attain the orthorhombic structure, the Pawley plots for monoclinic and orthorhombic are different. The positions of the patches of preferred orientation are the same but their populations of individual spots are different. In ideal crystals the ratio of the populations of spots in neighboring patches of Pawley projections should be 1:2 for the monoclinic structure and 1:1 for the orthorhombic. Figure 11 shows Pawley projections of the final configurations of clusters at 130 K together with the population ratios for several clusters. For cluster no. 1 this ratio is close to 1:2, according to direct counts from an nlarged Pawley projection, signifying a monoclinic structure, while for clusters no. 2 and no. 3 the ratios are close to that for an orthorhombic phase. For some of the clusters, however, the ratio is 1:1.4 or 1:1.5, values that do not correspond to either of the ideal

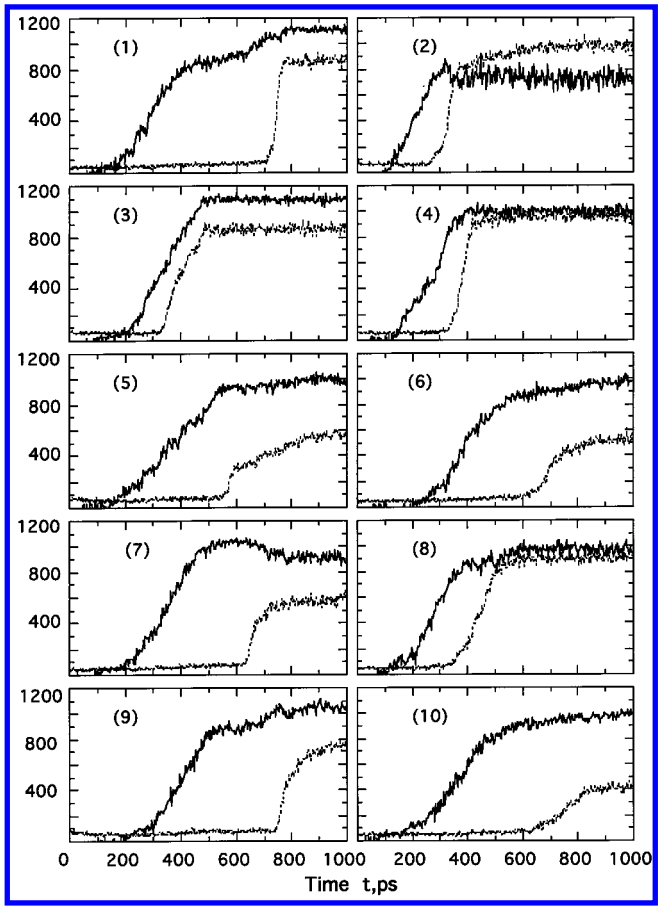

Figure 10. Same as in Figure 9 except at 130 K.

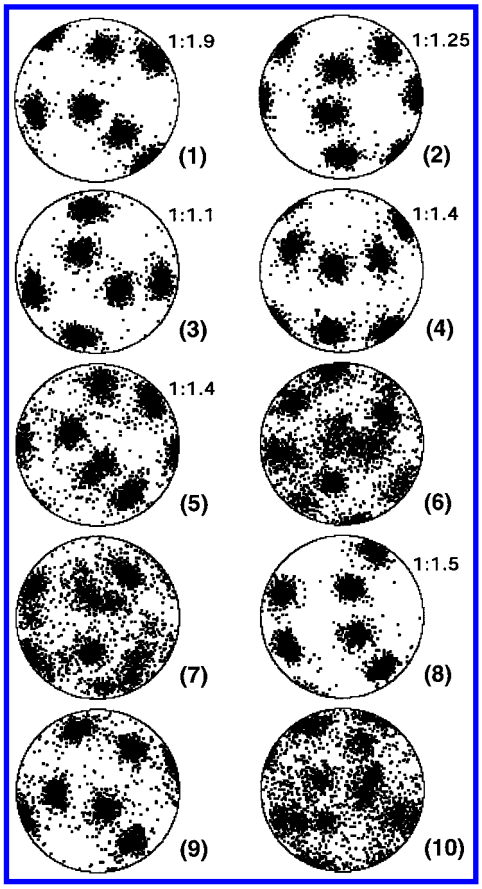

Figure 11. Pawley projections of the core molecules in final configuration for the 1722-molecule clusters at 130 K. The sharpness of the patches of points in comparison with those of the bcc (Figure 5) shows that all clusters are frozen to low-energy forms but the polycrystalline nature of many clusters is also evident.

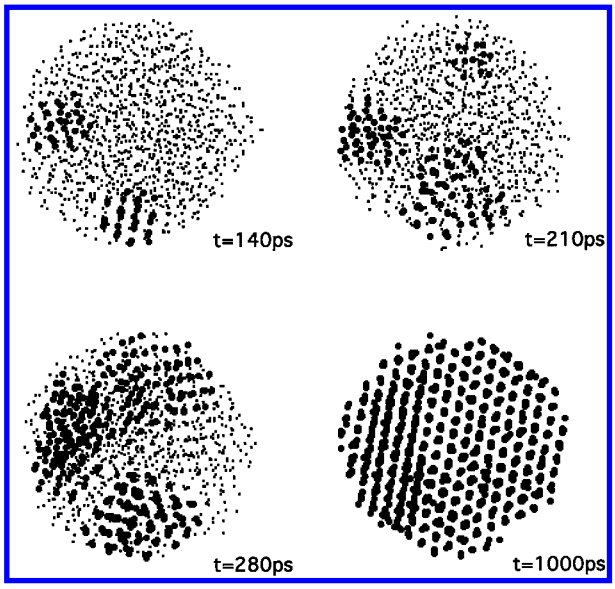

Figure 12. Snapshots of the centers of mass of core molecules in 1722-molecule cluster no. 1 during crystallization at 140 K.

structures. Two factors may account for such ratios. First of all, the analyses of clusters' growth and final configurations clearly indicate the presence of polycrystalline aggregates and a mixture of structures may arise. Second, ratios 1:2 or 1:1 correspond to infinite crystals. In the case of our clusters with free boundaries, the ratio may depend on finite size effects including the lack of an integral number of unit cells and the more haphazard orientations of molecules in grain boundaries and surface.

In Figure 12 we present a series of snapshots of molecules positions in cluster no. 1 during its freezing at 140 K. Only the core molecules are included in these plots. As in the 725-molecule plots, molecules in crystalline nuclei are represented by heavy dots to distinguish them from the other molecules. These nuclei appear to be compact because our criterion for bulklike solid molecules neglects the more poorly organized interfacial molecules that are also solidlike, based on their Voronoi polyhedra. Such molecules would have contributed to a more ramified appearance of nuclei, had they been highlighted, too. After 140 ps, two nuclei are observed. In the next snapshot 70 ps later, these two nuclei have grown in size and a third nucleus has appeared some distance away from the first two. Inasmuch as the cluster grew from several disconnected nuclei, the final structure is polycrystalline. Polynuclear growth was observed for all of the 1722-molecule clusters for reasons discussed in the next section.

A second observation illustrated in Figures 8 and 12 is that nuclei almost always formed near the surface of the cluster instead of in the interior. This was surprising to us because, when heating clusters in prior studies, we had always found that their surface layers melted at lower temperatures than the interior. Therefore, we supposed that the more disordered surface was so much less likely to be the site of nucleation to a crystal that we routinely subtracted the volume of the surface layer from the total volume when we computed rates of nucleation in MD runs. Clearly, this was wrong. One factor favoring nucleation near the surface would be the greater freedom of motion and, hence, a larger nucleation prefactor. It is not clear that this, by itself, can overcome the tendency for surface

molecules to avoid a rigid geometric regularity. A similar behavior of crystallization at or near the surface has also been reported for molecular dynamics simulations of the freezing of copper[22] and of NaCl[23] clusters.

Solid-State Transformation. The final bcc configurations of cluster no. 1 with 725 molecules and of no. 4 with 1722 molecules were additionally equilibrated for 40 000 time steps at 140 K generating starting sets of configurations for the investigation of the solid-state transition in a way analogous to that for freezing. Production runs were carried out at 130 K. During the 560 ps only 4 of the 12 of 725-molecule clusters underwent a solid-state transition as did 2 of the 10 of 1722-molecule clusters during the 350 ps of runs. All four of the smaller clusters that exibited a solid-state transition transformed to the monoclinic structure while, for those of the larger clusters which transformed, one became monoclinic and the other orthorhombic. On the other hand, in the case of freezing from the supercooled liquid state at 130 K, all clusters of both sizes ultimately transformed to the low-energy phase after passing through the bcc structure.

We suggest a possible reason for the striking differences between the clusters' ability to undergo a solid-state transition under the different starting conditions. When the supercooled liquid clusters froze at 130 K, they generally began to form a monoclinic nucleus before the freezing to the bcc structure was fully complete. The boundary between the solid and liquid phases (and grain boundaries in the case of larger clusters) constitutes inhomogeneous regions. The higher molecular mobility and fluctuations associated with these inhomogeneities could facilitate nucleation to the low-energy structure. It is worth noting that the final configurations of those larger clusters which began as single bcc crystals and transformed to the low-energy phase were perfectly monocrystalline. This manifestation of the lower solid-state nucleation rate in a homogeneous crystal is in contrast to the higher rate in the heterogeneous structures occurring when clusters were frozen from the supercooled liquid state.

Discussion

Mononuclear vs Polynuclear Transformations. As shown by Kashchiev et al.,[24] whether the crystallization in a given region is mononuclear or polynuclear depends on the volume V_m under observation and the ratio between two basic kinetic parameters, the growth rate and the nucleation rate. If growth of the first postcritical nucleus is fast enough, there is insufficient time for a second nucleus to form and the transition is said to be mononuclear. If several nuclei appear in the examined volume, the transition is polynuclear. Of course, the heat evolved in the transition may discourage further nucleation in the region, especially in small clusters. Kashchiev et al. have quantified the above idea in the case for which the degree of supersaturation is kept constant. These authors demonstrate that for a transition to be mononuclear, the volume, V, of the system must fulfill the inequality

$$V \ll (V_m/V)^{-1/4}(G/J)^{3/4} \tag{4}$$

where G is the linear growth rate of a nucleus, J is the nucleation rate (nuclei per unit time per unit volume), and V/V_m is unity for clusters. A failure to satisfy this inequality may result in polynuclear growth. In simulations, the nucleation rate was found to be $6._2(23) \times 10^{34}$ m^{-3} s^{-1} for the 725-molecule clusters and $8._1(34) \times 10^{34}$ m^{-3} s^{-1} for the 1722-molecule clusters, both at 140 K. If the growth rate is taken to be 12.4 m s^{-1} (see next section) for both sizes, the left-hand and right-hand quantities corresponding to the inequalities of eq 4 become

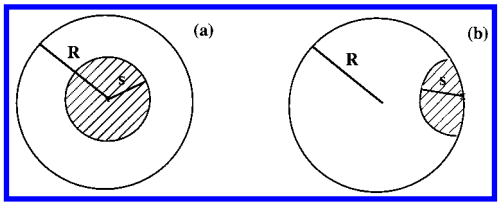

Figure 13. Schematic diagram of models of crystal growth corresponding to (a) eqs 5−8 treating nucleation in the interior and (b) eqs 9−14 treating surface nucleation in clusters

for the 725-molecule cluster:

$$V = 7.96 \times 10^4 \text{ Å}^3 > 5.3 \times 10^4 \text{ Å}$$

for the 1722-molecule cluster:

$$V = 18.9 \times 10^4 \text{ Å}^3 \gg 4.4 \times 10^4 \text{ Å}$$

Therefore, it might be concluded that polynuclear growth is likely in the freezing of both sizes of cluster, and rather more likely for the larger cluster. This size dependence in tendency was observed in the simulations but the fact that *all* of the smaller clusters froze to single crystals is not well accounted for by the inequality of eq 4. This result, by itself, does not argue against the validity of Kashchiev's criterion. The fact that single crystals were found for the smaller, completely frozen clusters does not demonstrate that the freezing was mononuclear. In our simulations it has often occurred that independent nuclei with different crystalline orientations merge as they grow, and adjust to each other as their molecules oscillate and shake each other until their crystalline orientations match. In a larger cluster, nuclei are more likely to grow beyond this malleable stage before they grow into each other. Another factor making clusters imperfect candidates for testing the criterion is that, for small clusters, no unique value of J exists for substitution into eq 4. The nucleation rate seems to be site-dependent, being greater near the surface than in the interior of a cluster.

Surface vs Interior Nucleation. If a cluster freezes by the growth of a single nucleus, the amount d$V(t)$ of supercooled liquid that is transformed over any short time interval depends on whether the nucleus is in the interior of the cluster or at the surface. We consider now the time dependence of the transformed volume for these two different idealized cases.

Case 1. Nucleation in the Interior of a Cluster. Let us consider a nucleus of vanishing initial size that appears at time $t = 0$ at the center of a spherical cluster with radius R (Figure 13a). Let us assume (1) that the nucleus grows isotropically as a sphere with the radius $s(t) = G \times t$ and (2) that the growth rate G is time-independent. The volume fraction $X(t) = \text{d}V(t)/V$ transformed under these conditions can be written as[25]

$$X(t) = 1 - \exp\left(-\frac{\pi}{2}\tau^3\right) \tag{5}$$

Here τ is a dimensionless measure of time

$$\tau = \frac{s(t)}{R} = \frac{G}{R}t, \quad 0 < \tau < 1 \tag{6}$$

Equation 5 is a particular form of a classical Kolmogorov−Johnson−Mehl−Avrami equation[26−28] for isothermal nucleation and growth transformation and

$$X(t) = 1 - \exp(-Ct^n) \tag{7}$$

where the constant C and value of n depend on the system or model under study. Next, we assume that at time $t = 0$, N nuclei of the solid phase are simultaneously generated at random positions in the interior of the cluster. Following nucleation, growth takes place, again in a spatially isotropic manner, with the same growth rate for all nuclei. When any of two growth fronts impinge upon each other, growth ceases along their common interface but continues elsewhere. The fraction of transformed volume $X(t)$ is then given by

$$X(t) = 1 - \exp\left(-\frac{\pi}{2}N\tau^3\right) \tag{8}$$

Case 2: *Surface Nucleation (Figure 13b)*. All the assumptions are the same as for nucleation in the interior except, for this case, N nuclei are randomly distributed on the surface of a spherical cluster. Following such assumptions, the fraction of transformed volume can be expressed as[29]

$$X(\tau) = 1 - (1-\tau)^3 - \sum_{i=0}^{N}\binom{N}{i}(1-\tau^2)^{N-1}\sum_{j=0}^{N}F(1-\tau;i,j) \tag{9}$$

for $0 < \tau < 1$, or

$$X(\tau) = 1 - \sum_{i=0}^{N}\binom{N}{i}(1-\tau^2)^{N-1}\sum_{j=0}^{N}F(1-\tau;i,j) \tag{10}$$

for $1 < \tau < 2$, where

$$F(x;i,j) \equiv \frac{3}{2^{2N-1}}\binom{i}{j}\frac{1-x^{2i-j+3-N}}{2i-j+3-N} \tag{11}$$

for $j \neq 2i + 3 - N$, or

$$F(x;i,j) \equiv \frac{3}{2^{2N-1}}\binom{i}{j}(-\ln x) \tag{12}$$

for $j = 2i + 3 - N$. The binomial coefficients in (8−11) are

$$\binom{N}{n} \equiv \frac{N!}{n!(N-n)!} \tag{13}$$

For the special case $N = 1$, eqs 8−11 reduce to a simple result, obtained by Levi and Mehrabian[30]

$$X(\tau) = \frac{1}{2}\tau^3 - \frac{3}{16}\tau^4 \tag{14}$$

for $0 < \tau < 2$. Results of applying these equations were compared with results from the molecular dynamics simulations in the freezing of 1722-molecule clusters at 140 K. The best fit in such a comparison yields a value of the growth rate, G. The temperature of 140 K was selected because at that temperature the solid-state transition from bcc to monoclinic is well separated from the freezing transition, whereas the two transitions tend to overlap at 130 K and complicate the picture. Figure 14 presents the volume fraction transformed as a function of time for different clusters in comparison with predictions of the models of surface nucleation (solid lines) and of interior nucleation (dashed lines). MACSPIN[31] images as well as the present analysis show that cluster no. 4 at 140 K is the only one to freeze from a single nucleus. Although other nuclei appeared in this cluster during freezing, some of them dissolved back into the liquid while others that formed close to the main nucleus merged with it. The final configuration of this particular cluster had a perfect bcc structure. That might be the reason

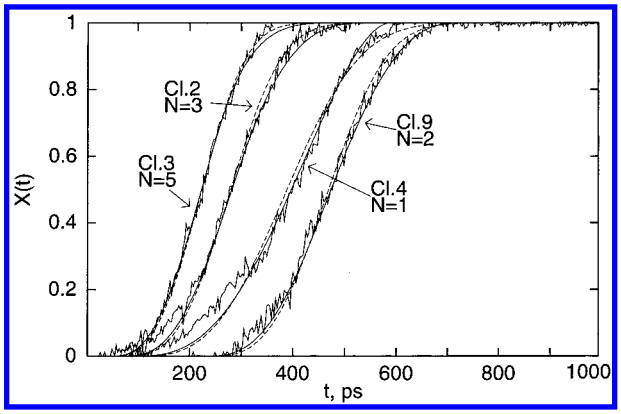

Figure 14. Volume fraction transformed as a function of time for different 1722-molecule clusters at 140 K in comparison with fitted curves corresponding to the models of surface nucleation (solid lines) and interior nucleation (dashed lines).

why this cluster remained in the bcc phase while all the other clusters in the simulations ultimately transformed to the monoclinic phase. Perhaps the grain boundaries in the other clusters (which were all polycrystalline) were associated with distortions and stress that catalyzed the (therefore heterogeneous) nucleation to the low-temperature phase.

The number density of clusters in bcc phase was estimated to be 0.0095 $Å^{-3}$, making the cluster radius approximately 31 Å. Since the duration of freezing in this cluster was approximately 500 ps, the growth rate would correspond to 6.2 m s^{-1} if the nucleus began in the center of the cluster, or 12.4 m s^{-1} if it began at the surface. Growth rates derived from the best fitting of eq 5 or eq 14 for $R = 31$ Å agree with the simple estimate, being 6.2 and 12.4 m s^{-1}, respectively. Furthermore, the same growth rate was used successfully in the surface nucleation model for all other clusters with different numbers of nuclei N. On the other hand, for the interior nucleation model, the best fits resulted when a growth rate decreased slightly as the number of nuclei, N, increased. For example, G was 5.8 m^{-1} s^{-1} for cluster no. 3 with $N = 5$ (see Figure 14)

For comparison with the MD results is the growth rate of 13.1 m s^{-1} predicted by Turnbull's theory of growth[32] (see the Appendix). A similar but somewhat smaller value is obtained via the Wilson−Frenkel theory.[33] Of course, all of the models for the kinetics of growth are oversimplified. Especially large disagreements are observed in Figure 14 at the beginning of crystal growth due to the assumption of vanishingly small nuclei. Nevertheless, from the present investigation we conclude that the kinetics of freezing of large SeF_6 clusters is better represented by a model of surface nucleation model than by one with nucleation in the interior. Although the evidence cited directly above is, at best, rather weak, the images from molecular dynamics simulations are quite compelling.

Critical Nuclei. A few words should be said about the size of critical nuclei. In our simulations, some embryos grew to 50−55 bulklike crystalline molecules but then dissolved again into the liquid phase. Therefore, we conjecture that the size of critical nucleus is probably not much smaller than 55 molecules at 130 K. This is an order of magnitude larger than forecast by the classical theory on the basis of the nucleation rates we encounter.[2] Moreover, our estimate totally neglects the many molecules at the liquid-crystal interface which pass the Voronoi test but not the bulklike criterion. Just how these molecules should be apportioned between the nucleus and the surroundings may be clarified by studies of the profiles of order parameters such as density, translational, and orientational order of

TABLE 2: Thermodynamic and Physical Properties Adopted in the Appendix[a]

quantity	value	ref
T_m, K	238	15, 16
ΔH_f, kJ mol^{-1}	7.1	34
D, m^2 s^{-1}	$1.23 \times 10^{-10} \exp(-842/T)$	2

[a] Jump length λ was chosen to be a molecule diameter: $\lambda = 2r = 5.76$ Å.

molecules. The last order parameter is a new one in the study of phases at the molecular level because all prior investigations were of monatomic systems. A more detailed examination of such factors will be presented in the next paper.

Acknowledgment. This research was supported by a grant from the National Science Foundation.

Appendix

Applying absolute rate theory, Turnbull has shown[32] that the velocity of crystal growth in freezing can be approximated by

$$G = \frac{D\Delta H \Delta T}{\lambda R T T_m} \tag{15}$$

where D is the coefficient of diffusion, ΔH is the molar heat of fusion, λ is the molecular "jump" distance, R is the gas constant, T_m is the melting temperature, and ΔT is the degree of supercooling, $T_m - T$ (see Table 2). We have used the values of the thermodynamic and physical properties from Table 2 to calculate the growth rate at $T = 140$ K according to eq 15.

References and Notes

(1) Kinney, K. E.; Xu, S.; Bartell, L. S. *J. Phys. Chem.* **1996**, *100*, 6935.
(2) Santikary, P.; Kinney, K. E.; Bartell, L. S. *J. Phys. Chem.* **1998**, *102*, 10324.
(3) Chushak, Y.; Santikary, P.; Bartell, L. S. *J. Phys. Chem.* **1999**, *103*, 5636.
(4) Braune, H.; Knoke, S. *Z. Phys. Chem. Abt. B* **1933**, *21*, 297.
(5) Kinney, K. E. Ph.D. Thesis, University of Michigan, Ann Arbor, MI, 1995.
(6) Tanemura, M.; Hiwatari, Y.; Matsuda, H.; Ogawa, T.; Ogita, N.; Ueda, A. *Prog. Theor. Phys.* **1977**, *58*, 1079.
(7) Hsu, C. S.; Rahman, A. *J. Chem. Phys.* **1979**, *71*, 4974.
(8) Cape, J. N.; Finney, J. L.; Woodcock, L. V. *J. Chem. Phys.* **1981**, *75*, 2366.
(9) Powell, B. M.; Dolling, G. *Can. J. Chem.* **1988**, *66*, 897.
(10) Raynerd, G.; Tatlock, G. J.; Venables, J. A. *Acta Crystallogr.* **1982**, *B83*, 1896.
(11) Pawley, G. S.; Thomas, G. W. *Phys. Rev. Lett.* **1982**, *48*, 410; Pawley, G. S.; Dove, M. T. *Chem. Phys. Lett.* **1983**, *99*, 45.
(12) Fuchs, A. H.; Pawley, G. S. *J. Phys. (Paris)* **1988**, *49*, 41.
(13) Xu, S.; Bartell, L. S. *J. Chem. Phys.* **1993**, *97*, 13540.
(14) Xu, S. Ph.D. Thesis, University of Michigan, Ann Arbor, MI, 1993.
(15) Virlet, J.; Rigny, P. *Chem. Phys. Lett.* **1970**, *6*, 377.
(16) Michel, J.; Drifford, M.; Rigny, P. *J. Chim. Phys.* **1970**, *67*, 31.
(17) Gilbert, M.; Drifford, M. In *Advances in Raman Spectroscopy*; Mathieu, J. P., Ed.; Heyden and Sons: London, 1972; Vol. 1.
(18) Blinc, R.; Lahajnar, G. *Phys. Rev. Lett.* **1967**, *19*, 685.
(19) Dibble, T. S.; Bartell, L. S. *J. Phys. Chem.* **1992**, *96*, 8603.
(20) Boutin, A.; Rousseau, B.; Fuchs, A. H. *Chem. Phys. Lett.* **1994**, *218*, 122.
(21) Bartell, L. S.; Xu, S. *J. Chem. Phys.* **1995**, *99*, 10446.
(22) Valkealahti, S.; Manninen, M. *J. Phys.: Condens. Matter* **1997**, *9*, 4041.
(23) Huang, J., private communication.
(24) Kashchiev, D.; Verdoes, D.; van Rosmalen, G. M. *J. Cryst. Growth* **1991**, *110*, 373.
(25) Markworth, A. J. *Scr. Metall.* **1984**, *18*, 1309.
(26) Kolmogorov, A. N. *Bull. Acad. Sci. USSR, Div. Math. Nat. Sci.* **1937**, *3*, 355.
(27) Johnson, W. A.; Mehl, R. F. *Trans. Am. Inst. Mining Metall. Eng.* **1939**, *135*, 416.
(28) Avrami, M. *J. Chem. Phys.* **1939**, *7*, 1103; **1940**, *8*, 212; **1941**, *9*, 177.
(29) Markworth, A. J. *Mater. Sci. Eng.* **1988**, *100*, 169.
(30) Levi, C. G.; Mehrabian, R. *Metall. Trans. A* **1982**, *13A*, 221.
(31) MACSPIN, 3.01 ed.; Abacus Concepts Inc.: Berkeley CA, 1991.
(32) Cormia, R. L.; Mackenzie, J. D.; Turnbull, D.*J. Appl. Phys.* **1963**, *34*, 2239.
(33) Wilson, H. A. *Philos. Mag.* **1900**, *50*, 238; Frenkel, J. *Phys. Z. Sowjetunion* **1932**, *1*, 498.
(34) *American Institute of Physics Handbook*, 2nd ed.; Gray, D. E., Ed.; McGraw-Hill: New York, 1963; pp 4−208.